Bunsen flame analysis using simultaneous tomographic images and PIV in the fresh and burnt gases.

B. Jeanne, E. Samson, B. Renou and A. Boukhalfa

LAME - CORIA UMR 6614 CNRS
INSA - Avenue de l'Université - BP8
76801 Saint-Etienne-du-Rouvray Cedex
France

ABSTRACT

Particle Cross-correlation Image Velocimetry (PIV) technique, is used in order to measure simultaneously the instantaneous velocity field and the instantaneous flame front position with a high accuracy on laminar and low turbulent premixed flames stabilised at the exit of a Bunsen burner. The geometrical simplicity of those flames enables basic knowledge on laminar and turbulent combustion characteristics such as the flame speed, the curvature, the velocity field, and the flame stretch. A double seeding is required to determine precisely the flame front location and the instantaneous velocity field in the fresh and burnt gases. Indeed, when considering a tomographic image made with Zirconium oxide particles only, it is not possible to determine precisely the flame front location since the grey-level histogram does not show any threshold. Thanks to the use of incense smoke, the fresh gases area can be determined with accuracy. Flame contours are systematically extracted from the tomographic recordings using an automatic detection procedure of the threshold based on grey level histogram thresholding by index of fuzziness. Since the Zirconium oxide seeding density is sufficient for processing data both upstream and downstream the flame front position, the velocity field can be directly obtained. An improvement in the basic PIV technique is to separate the pair of PIV images according to the fresh and burnt gases since the flame contour position is determined with a high accuracy. Fresh and burnt gases are processed separately using a 'mask' in order to improve the accuracy of the PIV measurement. On top of that, this masking technique can reduce the influence of the measured velocity of the fresh gases, because the greater density of particle images on this side tends to dominate the correlation. The PIV calculation will be done in both regions, taking into account only the local phenomena and not the influence of the other side of the flame front. Thus, the local flame properties such the flame curvature, the flame speed and the flame stretch could be determined thanks to the coupling of the velocity field and the flame front location. That is why the accuracy and the simultaneousness in the measurements of the flame front location and the velocity field for both side of the flame are of first importance.

1. INTRODUCTION

Bunsen burner is a common tool to study laminar and turbulent flames properties (Echekki and Mungal, 1990, Muniz et al., 1994, Paone et al., 1994, Mungal et al., 1995). Zirconium oxide has been used in order to characterise those instantaneous velocity field (Muniz et al., 1994, Paone et al., 1994, Mungal et al., 1995), but the obtaining of the flame contour is more difficult. On the other hand, flame contours and then curvatures are frequently determined using tomography (Boyer, 1980, Chew et al., 1989, Deschamps et al., 1996, Renou et al., 1998). In this case, the tracer, like silicon oil, is introduced in the fresh gases and disappears at the entrance of the flame front, as well as the knowledge of the velocity field. In the present work, a method is presented to analyse with accuracy the flame properties such as the velocity field and the flame front location, which enable the knowledge of local flame properties.

2. EXPERIMENTAL SET-UP

Experiments are performed on laminar and low turbulent premixed flames stabilised on a Bunsen burner with a exit diameter of 30 mm. The premixed methane/air flame (equivalence ratio $\Phi = 1.1$) is stabilised by a methane/air pilot flame ($\Phi = 1.0$). The jet and the pilot flame sprung from two concentric tubes, 29 cm long, with a pilot internal and external diameter of 30 mm and 36 mm respectively. The mean jet velocity varies in order to obtain Reynolds numbers based on the exit diameter varying from 2000 to 5000 (Figure 1).

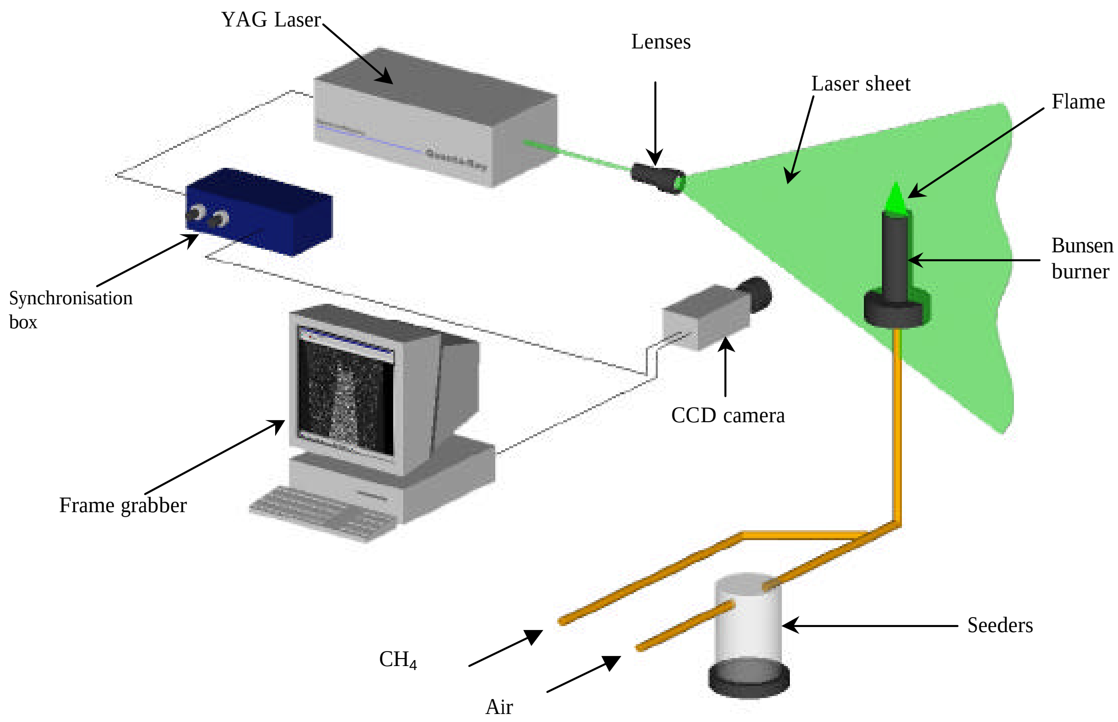

Fig. 1. Experimental set-up

The air flow is seeded simultaneously with metal oxide particles (ZrO_2) and incense smoke, obtained from combustion of incense cone-shaped. The incense particles which burned at the entrance of the flame front have been chosen to increase the contrast between the fresh and burned gas zones, on the tomographic recordings. Furthermore, these incense particles have been chosen for this application, because they present a mono-disperse fine distribution of particle size and they avoid agglomeration of solid particles.

The seeded flow is illuminated by a doubled-pulsed laser sheet. The light source is Nd:YAG 200mJ, Spectra-Physics PIV 200, with second harmonic generating crystals used to create a Q-switched laser output at 532 nm. The planar laser sheet is obtained by a combination of sperical-cylindrical lenses with a thickness in the middle of the test section closed to 500 μm.
Two successive flame images of the test section are recorded with a 50mm Nikkor lens (f:1/1.2) on a high resolution CCD camera (Kodak Megaplus ES1), with a CCD array of 1008 × 1018 pixels. Interrogation of the recorded PIV images is performed by two-dimensional digital cross-correlation analysis. The maximum location of the correlation peak is then determined by using a Gaussian subpixel analysis. A comparison will be made between the sampling window size : 32 × 32 $pixels^2$ with an overlapping of 50% and 64 × 64 $pixels^2$ with an overlapping of 75%, corresponding respectively to 2.35 × 2.35 mm^2 and 4.7 × 4.7mm^2 zone in real space.

3. EXPERIMENTAL RESULTS

3.1. Flame contour detection

Zirconium oxide particles are used to enable the determination of the velocity field in the fresh gases as well as in the burned gases. Due to the gas expansion through the flame, the seed density is much greater in the fresh gases than in the burnt gases. Then, when considering a tomographic image made with oxide particles only (Fig. 2a), it is not possible to determine precisely the flame front location since the grey level histogram (Fig. 2b) does not show any threshold. Nevertheless, an estimation of the flame front position can be obtained considering the mean pixel intensity calculated over a small area of image (Stevens et al., 1998). The size of this averaging area can then be considered as the critical parameter since large areas tend to smooth the trace of average intensity leading to greater error in the flame front position.

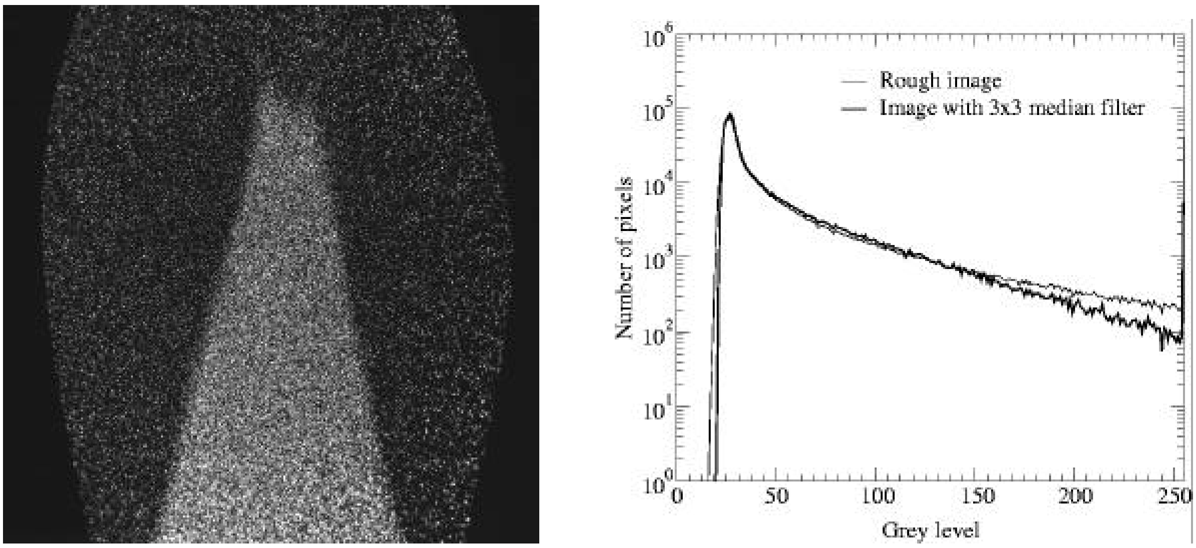

(a) (b)

Fig. 2. Seeded flame with only Zirconium oxide particles.
a) Tomographic image
b) Histogram with only Zirconium particles.

Thanks to the use of incense smoke, the fresh gases area location can then be determined with accuracy (Fig. 3a and 3b). The histogram of such an image hence reveals a threshold which enables to determine the flame front position with a high accuracy. The grey background in the fresh gases does not alter the cross-correlation analysis since the oxide particles present in the fresh gases appear with higher grey-level and are therefore well visible.
Flame contour are then systematically extracted from PIV recordings using an automatic detection procedure of the threshold based on grey level histogram thresholding by index of fuzziness. The algorithm ensures to detect the valleys of the histogram corresponding to the optimum threshold by minimizing the greyness ambiguity as reflected by the measures. This procedure detailed by Murthy and Pal, 1992, and, Lim and Lee, 1990, can be

divided in two parts: the histogram smoothing by the determination of the index of fuziness, and then the detection of the threshold by using the first and the second derivatives (Fig. 4).

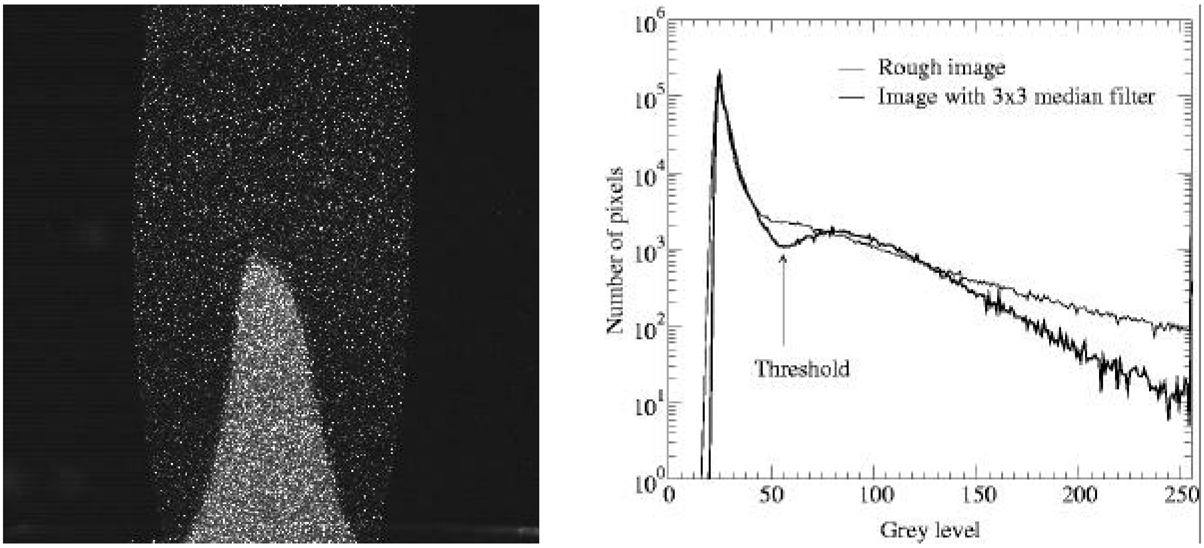

(a) (b)

Fig. 3. Seeded flame with Zirconium oxide particles and incense smoke.
a) Tomographic image
b) Histogram with Zirconium particles and incense smoke.

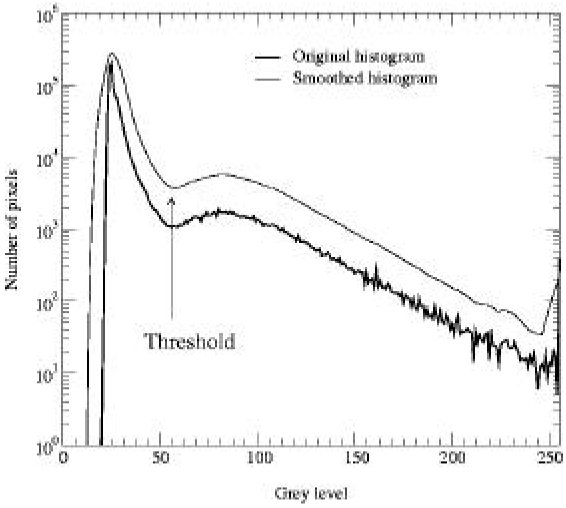

Fig. 4. Automatic thresholding procedure

Then, an edge-finding algorithm is adapted to obtain a continuous flame edge from each of the images. Once the contour is determined, it has to be interpolated in order to match as much as possible the real contour and to remove the pixelization noise. As a matter of fact, the determination of the flame front location depends on the presence or not of incense smoke particles, the information obtained is discrete and must be turned out into a continuous information. One way can be to use a polynomial interpolation to match as much as possible the real contour (Renou, 1999). This interpolation is made for each point of the contour, taking into account a certain number of neighbours. The number of points in each part as well as the degree of the polynomial are the two relevant parameters when interpolating the contour. The choice of those parameters can be done by direct comparison between the interpolated contour and the initial image. It can be also determined precisely by defining a convergence criterion in the evolution, for example, of the mean curvature as a function of contour parameters. The local flame curvature h is computed at each flame contour co-ordinate by using the following relation (Mokhtarian and Macworth, 1986):

$$h = \frac{dx}{ds}\frac{d^2y}{ds^2} - \frac{dy}{ds}\frac{d^2x}{ds^2} \Bigg/ \left(\left(\frac{dx}{ds}\right)^2 + \left(\frac{dy}{ds}\right)^2 \right)^{3/2} \quad (1)$$

where s is the curvilinear coordinate of the flame front. The sign convention used for the curvature measurement assigns positive values to regions convex to the burnt gases and negative values to regions convex to the reactant

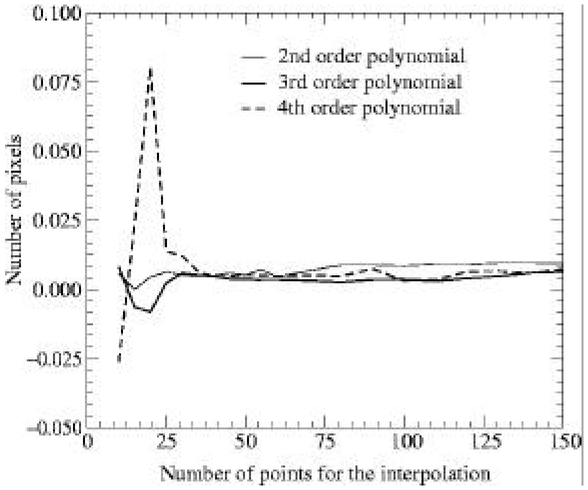

(a)

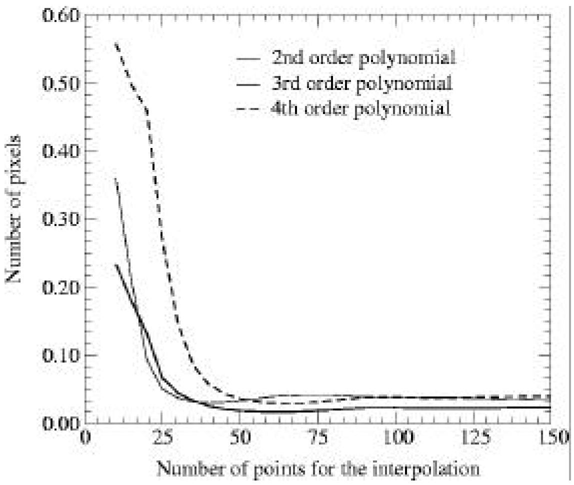

(b)

Fig. 5. Interpolation parameters.
a) Mean curvature of the flame front as a function of interpolation parameter
b) Standard deviation of the curvature of the flame front as a function of interpolation parameters

Figures 5a and 5b represent the evolution of the mean curvature and the standard deviation of curvature depending on the degree of the polynomial and the number of points used for the interpolation. One can remark that, if the number of points is too small, the curvature PDF highly depends on the parameters of interpolation. This can be explained by the fact that non physical curvature is generated by the interpolation. On the opposite, if the number of points is too high, the interpolated contour becomes too smoothed and does not match anymore the real contour. Therefore, the appropriate number of points of interpolation is chosen as the smallest value which give PDF characteristics independent of interpolation parameters (Fig. 6).

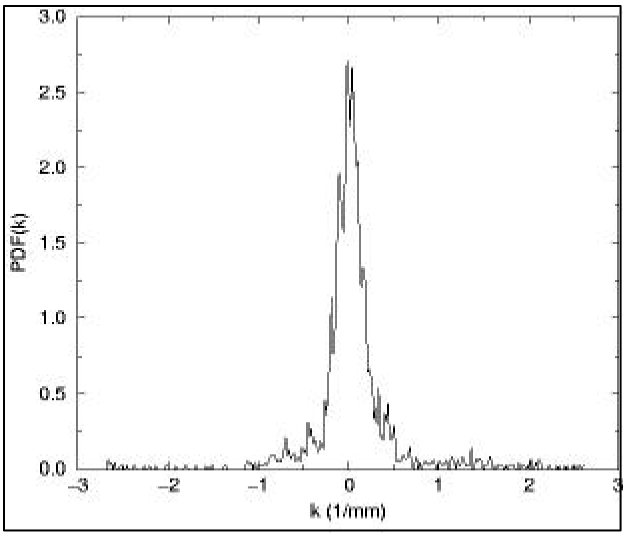

Fig. 6. Probability density function of curvature (k_{mean} = -0.017mm^{-1}, s_k = 0.20mm^{-1})

3.2. Simultaneous measurements of scalar field and velocity field.

Since the Zirconium oxide seeding density is sufficient for processing data both upstream and downstream the flame front position, the velocity field can be directly obtained (Figure 7). After the PIV calculations, several post-processing procedures are required. Spurious vectors are detected by an automatic validation procedure whereby the SNR of the correlation peak had to exceed a minimum value, and the vector amplitude had to be within a certain range of the local median to be considered as valid. Once spurious vectors have been detected, they are replaced by vectors resulting from a linear interpolation in each direction from the surrounding 3×3 set of vectors. Then, the velocity field is low-pass filtered, using a gaussian 3×3 filter, in order to reduce errors at each node and to calculate gradient quantities of the velocity field.

As described by previous experimental works (Mungal M.G. et al., 1995, Paone N. et al., 1994), the velocity vectors change significantly at the sides of the flame front since the normal component of the velocity increases for the volume expansion associated with the thermal expansion while the tangential component is conserved. The acceleration due to the flame front is obvious on the iso-colour representation. The comparison with the position of the flame contour determined simultaneously using incense smoke shows an acceleration of the velocity field after the flame front position, in the burnt gases. This phenomena can be explained by the particle slip due to the gas acceleration. Indeed, since PIV measures the velocity of particles in the flow rather than the fluid velocity, the accuracy of the measurements is critically depend upon well the seed particles follow the flow with strong acceleration. The difference between the gas velocity and the particle velocity near the hot side of the flame can reach 1m/s and decreases significantly when the flow acceleration becomes smaller.

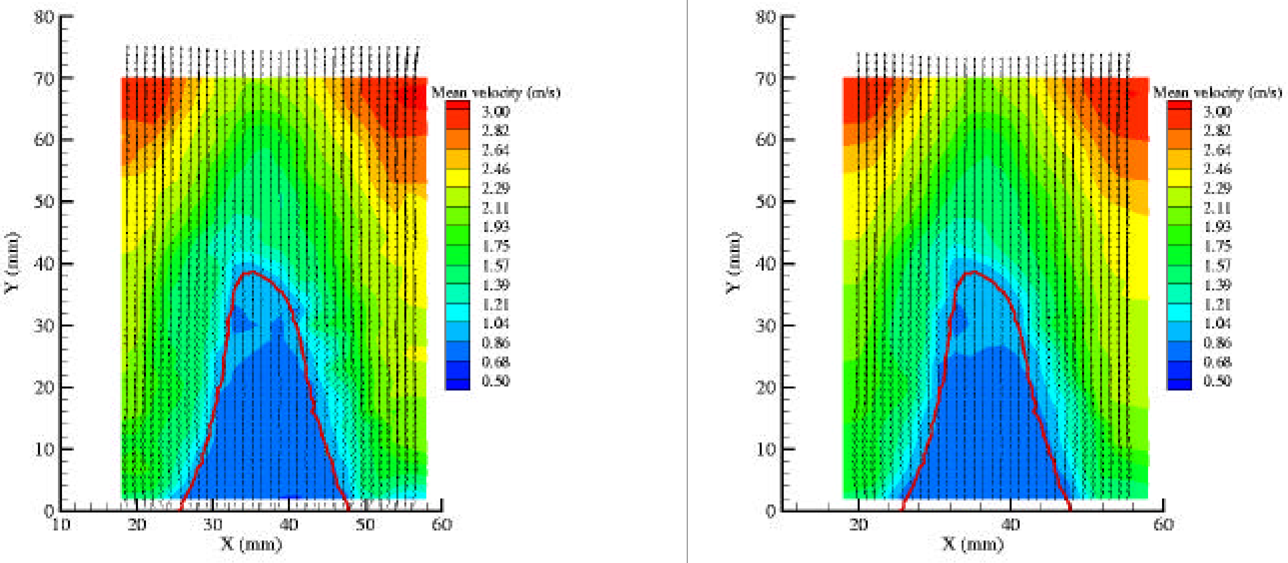

(a) (b)

Fig. 7. Simultaneous measurement of both scalar and velocity field for a laminar Bunsen flame.

a) 32´32 pixels^2, 50% overlapping, magnification ratio : 13.6 pixels/mm

b) 64´64 pixels^2, 75% overlapping, magnification ratio : 13.6 pixels/mm

Since PIV calculation makes a kind of averaging in the window, calculations done on the flame contour take into account both influences of fresh and burnt gases. Results are then automatically erroneous. One way to avoid this problem is to align the interrogation area along the flame front parallel to the flame, such that the almost exclusively reactant or product particle images exist in each interrogation area. Such a problem can also be resolved by the separation of the pair of PIV images according to the fresh and burnt gases, since the flame contour position is determined with a high accuracy (Fig. 8).

The PIV calculation will be done in both regions, taking into account only the local phenomena and not the influence of the other side of the flame front (Frank et al., 1996, Stevens et al., 1998). Indeed, this masking technique can reduce the influence of the velocity of the fresh gases, because the greater density of particle images on this side tends to dominate the correlation. That is, there were no large difference between neighbouring vectors on the same side of the flame, while there were significant changes in velocity across the flame.

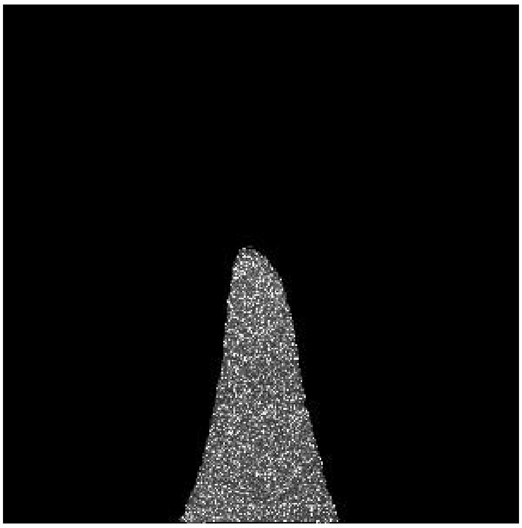

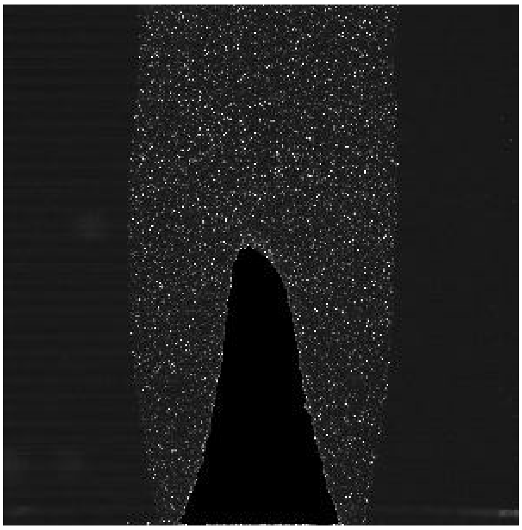

(a) (b)

Fig. 8. Separation of the PIV images
a) in a 'fresh' part
b) in a 'burnt' part

In such a way, on a same PIV window located on the flame front, one can find two vectors. Then, they are displaced to be located in the gravity centre of the image part used for the PIV calculation (Fig. 9).

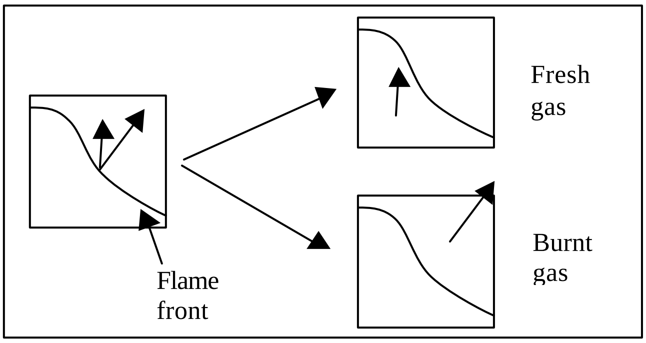

Fig. 9. Decomposition of the flow field into two parts : one for the fresh gas, one for the burnt gas.

A limitation on the size of the computing window can be made regarding the percentage of the mask in the interrogation area. Here, 50% of the original size is required to validate the calculation since the correlation peak becomes undetectable with accuracy because of its "roof shape". Figures 10a and 10b represent the velocity field obtained with this masking technique and can be directly compared with the initial velocity field. The phenomena in front and in back of the flame are then separated. The better resolution of the discontinuity of the flow field across the flame can then be quantified looking at the radial component of the flow (Fig. 11a and 11b). The decomposition of the PIV calculation erases the problem of smoothing on the flame contour, since great gradients are present in this area.

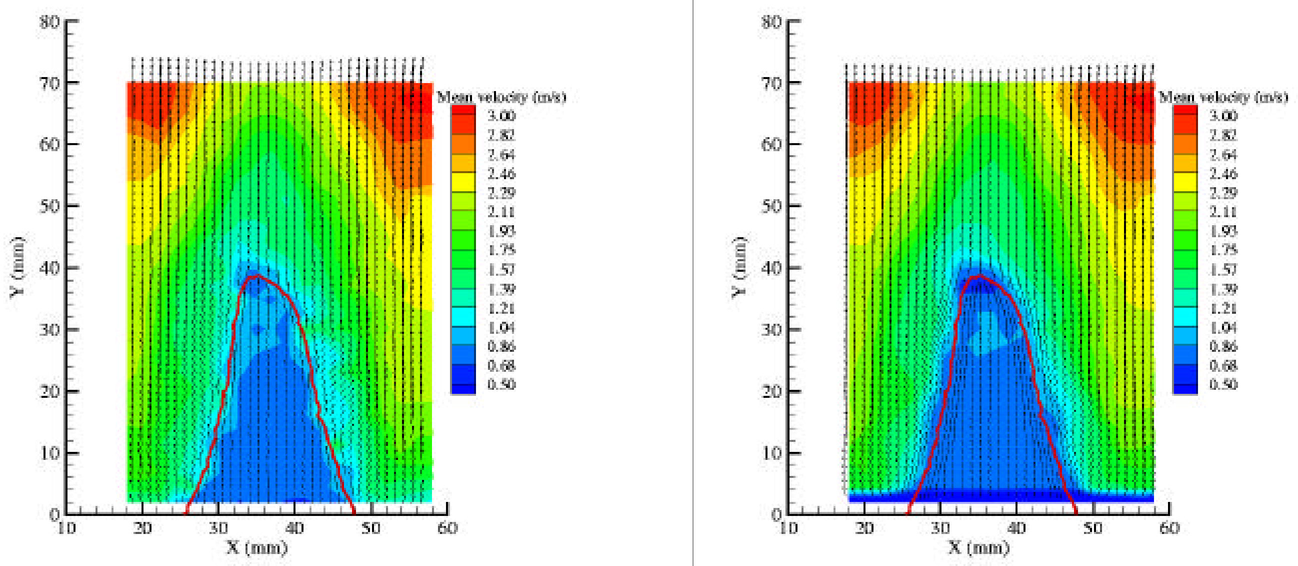

(a) (b)

Fig. 10. Simultaneous measurement of both scalar and velocity field for a laminar Bunsen flame using the decomposition technique into two zone of calculation
a) 32´32 pixels^2, 50% overlapping, magnification ratio : 13.6 pixels/mm
b) 64´64 pixels^2, 75% overlapping, magnification ratio : 13.6 pixels/mm

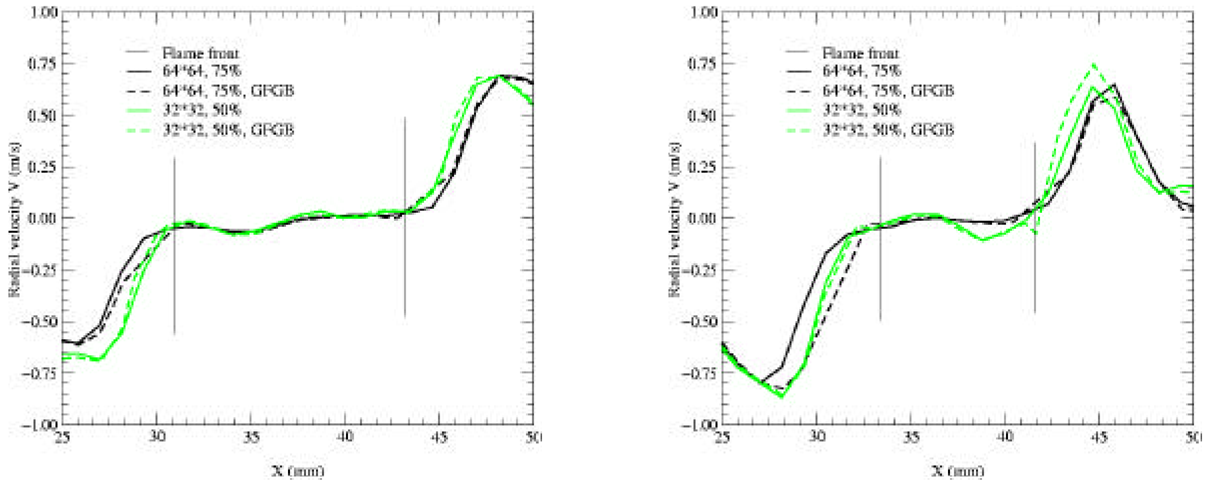

(a) (b)

Fig. 11 Radial velocity profile (BG/GF corresponds to the decomposition method)
a) at Y = 12 mm
b) at Y = 26 mm

CONCLUSION

A method has been presented to analyse simultaneously with accuracy the flame properties such as the flame front location and the velocity field in both fresh and burnt gases. An improvement in the basic PIV technique is to separate the pair of PIV images according to the fresh and burnt gases since the flame contour position is determined with a high accuracy. Fresh and burnt gases are processed separately using a 'mask' in order to improve the accuracy of the PIV measurement an to reduce the influence of the velocity of the fresh gases on the burned gases. The PIV calculation will be done in both regions, taking into account only the local phenomena and not the influence of the other side of the flame front. Thus, the local flame properties and the flow field characteristics could be determined thanks to the coupling of velocity field / flame front. That is why the accuracy and the simultaneousness in the measurements of the flame front location and the velocity field for both side of the flame are of first importance.

REFERENCES

[1]. Echekki T. and Mungal M.G., (1990), Twenty-Third Symposium (International) on Combustion, The Combustion Institute, pp. 455-461

[2]. Muniz L., Martinez R.E. and Mungal M.G., (1994), Seventh International Symposium on Applications of Laser Techniques to fluid mechanics, Lisbon, pp. 3.3.1-3.3.6

[3]. Paone N., Revel G.M. and Nino E., (1994), Seventh International Symposium on Applications of Laser Techniques to fluid mechanics, Lisbon, pp. 3.4.1-3.4.8

[4]. Mungal M.G., Lourenco L.M. and Krothapalli A., (1995), Combustion Science and Technology, Vol. 106, pp. 239-265

[5]. Boyer L., (1980), Combustion and Flame, Vol. 39, pp. 321-323

[6]. Chew T.C., Britter R.E. and Bray K.N.C., (1990), Combustion and Flame, Vol. 80, pp. 65-82

[7]. Deschamps B.M., Smalwood G.J., Prieur J., Snelling D.R. and Gülder Ö.L., (1996), Twenty–sixth Symposium (International) on Combustion, The Combustion Institute, pp. 427-435

[8]. Renou B., Boukhalfa A., D. Puechberty and Trinité M., (1998), Twenty-Seventh Symposium (International) on Combustion, The Combustion Institute, pp. 841-847

[9]. Stevens E.J., Bray K.N.C. and Lecordier B., (1998), Twenty-Seventh Symposium (International) on Combustion, The Combustion Institute, pp. 949-955

[10]. Murthy C. and Pal S.K., (1992), Information sciences, Vol. 60, pp. 107-135

[11]. Lim Y.W. and Lee S.U., (1990), Pattern Recognition, Vol. 22, pp. 935-952

[12]. Renou B., (1999), PhD Thesis, Université de Rouen, France.

[13]. Mokhtarian F. and Macworth A., (1986), IEEE transactions on pattern analysis and machine intelligence, PAMI-8, N°1, pp. 34-43

[14]. Frank J.H., Lyons K.M. and Long M.B., (1996), Combustion and Flame, Vol. 107, pp. 1-12

ACKNOWLEDGEMENTS

The authors would like to thank N. Fradet and M. Baluteau (I.N.S.A. Engineers, EP-2001), for their contribution to this experimental work.